ESR in layer-substrate structures: The line shape and nondestructive contactless measurements of the layer conductivity

V. Zevin
Racah Institute of Physics, The Hebrew University of Jerusalem, Jerusalem 91904, Israel

J. T. Suss
Solid State Physics Department, Soreq Nuclear Research Center, Yavne 70600, Israel
(Received 5 May 1986)

The electron-spin resonance of spins in a substrate may be used as a tool for investigating the electrical properties of a metallic (semiconducting) layer. This is accomplished by passing a microwave field through the layer into the substrate and detecting the distortion of the ESR line shape caused by the layer. This distortion depends upon the thickness and the conductivity of the layer, both of which may be obtained if the theoretical line shape of the ESR in such a structure is known. The theoretical line shape and the intensity of the ESR in a layer-substrate system are discussed for various pairs of layers and substrates (metal-metal, semiconductor-insulator, etc.) in the case of localized spins. The structure of the electromagnetic field in the sample is dependent upon the orientation of the constant external magnetic field with respect to the surface of the sample, but magnetic losses and the line shape do not change essentially as a function of the orientation. It is shown that the A/B ratio of the ESR line may be used for measuring the layer conductivity and/or layer thickness. An experiment in which Ge layers on a ruby substrate were studied at various temperatures is described here. Experimental data of A/B ratios are presented and layer conductivities as deduced from these ratios are in good agreement with the conductivities obtained by four-contact measurements. Possible applications of the method are discussed.

I. INTRODUCTION

The effect of a near-surface metallic layer on the ESR of localized spins which were spread both in the layer and in the metallic substrate has been studied previously.[1,2] In the work of Raizman *et al.*[1] the near-surface layer in the *Au*Er system was formed by metallurgical treatment of the alloy, and it was the study of the ESR line shape of Er spins which permitted the discovery of the metallic near-surface layer. The above-cited research[1,2] led to the investigation of the possibility of using the ESR of localized spins of a substrate to study conductivity properties of a layer which may be created artificially on a substrate (see Sec. III).

The main idea of the investigation of conducting properties of layers by means of the ESR signal from the substrate is based on the use of the ESR line shape as a tool responding both to the thickness and the conductivity of the layer. To implement this idea we suggest using either an insulator or a metal with diluted localized spins of impurities as a source of the ESR signal. In the absence of the layer, the line shape of the bulk (substrate) ESR signal is experimentally known. In many cases also the theoretical line shape of the ESR signal of the substrate has been treated: Either the Gaussian or the Lorentzian (or a combination) for the insulating substrate and the Dysonian form for the metallic case. When the substrate is covered with a conducting layer and both the geometry of the cavity and the special experimental arrangements (Sec. III) permit the microwave field to penetrate into the substrate only through the layer, the distortion of the ESR signal of the substrate is a detectable feature. Then this distortion is used to obtain the conductivity and/or the thickness of the layer (the former at microwave frequencies and in a constant magnetic field of the order of 1000—3000 Oe; regarding the possibility of reducing the constant magnetic field almost to zero, see Sec. IV). Of course the thickness of the layer cannot be very large compared to the penetration depth of the layer (the skin depth in the case of the metallic conductivity). In this sense an insulating substrate provides much more sensitivity because of its large ESR signal. On the other hand, very thin layers will cause a small deformation of the ESR line which would not be detectable.

To obtain the ESR line shape one has to calculate the magnetic losses in the system. It would be very difficult and very cumbersome to calculate losses in the cavity due to the layer-substrate sandwich placed in the maximum of the rf magnetic field of the cavity. Instead we calculate the specific surface impedance in the framework of a model in which the sample has planar symmetry and is wide enough to justify the use of infinite planes as boundaries. We assume that the microwave field on the upper surface of the layer is fixed during a sweep across the line and the reflection mode of the ESR is used. The procedure for obtaining the surface impedance in the case of the normal skin effect is analogous to that developed in work previously reported[3,4] for a homogeneous sample and the conduction-electron-spin resonance (CESR). This procedure uses Maxwell's equation together with the magnetization equation and appropriate boundary conditions. These boundary conditions make the main difference be-

tween our "sandwich" case and the homogeneous case. In addition, we investigate the influence of the dc magnetic field orientation on the microwave field and magnetic losses in media.

The case of the anomalous skin effect is much more complicated and in some cases may be treated as in the work of Lampe and Platzman.[5] But it seems that this case is unsuitable for obtaining simple, quantitative information about the layer by the ESR method.

This paper is organized as follows. In Sec. II the surface impedance of a layer-substrate system is obtained and magnetic losses are presented via the superposition of the absorption and the dispersion parts of the dynamical magnetic susceptibility of the substrate. A semiconductor-insulator and a metal-metal case are emphasized. Details and formulas for the case when the layer resonance also responds to the electromagnetic microwave field may be found in the Appendixes. Section III presents the experiment in which conductivity of layers on a ruby substrate was measured by means of the A/B ratio of the ESR signal of Cr^{3+}, yielding results in good agreement with four-probe conductivity data. Discussions and conclusions are in Sec. IV, where various possible applications of the method are discussed.

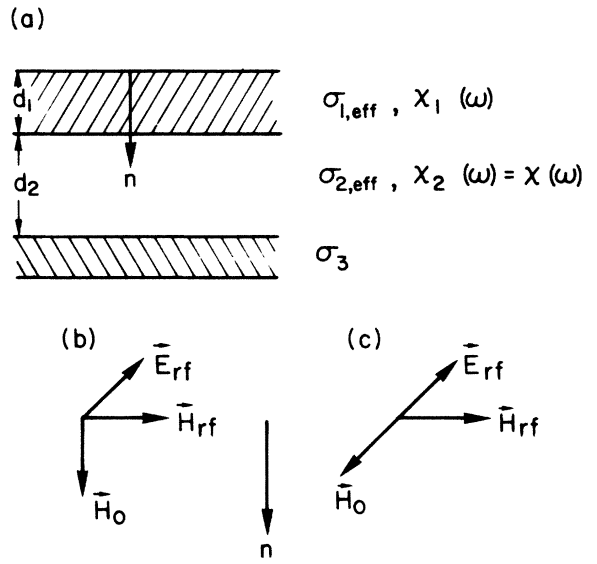

FIG. 1. (a) The geometry of the layer-substrate system. Indices 1 and 2 refer to layer and substrate, respectively. Index 3 refers to the metal plate. (b) and (c) are the two different geometries of the rf electromagnetic fields and the dc magnetic field with respect to the normal of the layer.

II. THEORY: THE ESR LINE SHAPE OF LOCALIZED SPINS IN A LAYER-SUBSTRATE SYSTEM

A. General considerations

In ESR experiments the external dc magnetic field $\mathbf{H}_0$ is kept perpendicular to the microwave rf magnetic field $\mathbf{H}$, but its orientation to the sample may be varied. Because the field $\mathbf{H}_0$ makes a magnetic medium anisotropic for the microwave field,[6] and because we are dealing here with the inhomogeneous medium [Fig. 1(a)] where reflections from inner boundaries determine in an essential way the shape and intensity of the ESR signal, there is a need to investigate the influence of the orientation of the field $\mathbf{H}_0$ upon magnetic losses. In what follows we assume the planar configuration of Fig. 1 where the effective conductivity is equal to

$$\sigma_{i,\text{eff}}=\sigma_i-\frac{i\omega\epsilon_i}{4\pi}, \quad i=1,2 , \tag{1}$$

where σ is the ohmic conductivity, ϵ the dielectric permittivity, and ω the microwave-field angular frequency. Indices 1 and 2 correspond to the layer and the substrate, respectively, and $\overleftrightarrow{\chi}_i(\omega)$, is the magnetic susceptibility tensor. In the case when the response of the layer spins to the microwave field is negligible, $\chi_1(\omega)=0$. This condition is justified either if there is a large enough difference between the g factor of localized spins in a substrate and the g factor of spins in a layer or if the layer spin resonance is a very broad one. Here we are mainly interested in the case when $\chi_1(\omega)=0$ (for $\chi_1(\omega)\neq 0$ see Appendix C).

We suppose that the microwave field is in the plane of the sample and that the magnetic component of this field on the upper boundary (Fig. 1) is fixed. The surface impedance is obtained by calculating the normal component of the Poynting vector $\mathbf{S}$ on the layer side of the upper surface. We have

$$\bar{S}_n=\frac{c}{4\pi}\overline{\mathbf{E}_{\text{real}}\times\mathbf{H}_{\text{real}}}\cdot\hat{\mathbf{n}}\,|_{n=0^+} , \tag{2}$$

where $\hat{\mathbf{n}}$ is the unit vector to the layer surface oriented into the system. The bar indicates the time averaging (we use the symbols H,E without subscript for the complex representation of the rf field).

To investigate the dependence of the microwave field upon the orientation of H_0 we are looking for the solution of Maxwell's equations for a media whose effective dielectric permittivity tensor is equal to

$$\overleftrightarrow{\epsilon}_{\text{eff}}=\overleftrightarrow{\epsilon}+\frac{i4\pi}{\omega}\overleftrightarrow{\sigma} \tag{3}$$

and the magnetic permeability tensor $\overleftrightarrow{\mu}$ is anisotropic due to the presence of the field $\mathbf{H}_0$. Choosing the z axis along the dc field $\mathbf{H}_0$, we obtain for the mutually perpendicular $\mathbf{H}$ and $\mathbf{H}_0$ fields[6]

$$\overleftrightarrow{\mu}=\begin{vmatrix}\mu_{xx} & \mu_{xy} & 0\\ \mu_{yx} & \mu_{yy} & 0\\ 0 & 0 & \mu_{zz}\end{vmatrix} , \tag{4}$$

with

$$\overleftrightarrow{\mu}=\overleftrightarrow{1}+4\pi\overleftrightarrow{\chi}$$

and

$$\chi_{yy}=\chi_{xx}, \quad \chi_{xy}=-\chi_{yx} . \tag{5}$$

In the case when the solution is in the form $\propto e^{-i(\omega t-\mathbf{k}\cdot\mathbf{r})}$, with $\mathbf{k}$ the complex wave vector, Maxwell's equations yield the expression[7]

$$\mathbf{k}\times\overleftrightarrow{\epsilon}_{\text{eff}}^{-1}(\mathbf{H}\times\mathbf{k})=\frac{\omega^2}{c^2}\overleftrightarrow{\mu}\,\mathbf{H}\ . \tag{6}$$

This equation determines possible vectors $\mathbf{k}$. In the case of the scalar permittivity ϵ_{eff} and the tensor $\overleftrightarrow{\mu}$ from Eqs. (4) and (5) with $\mu_{zz}=1$, we obtain from Eq. (6) the following compatibility equation

$$\begin{vmatrix} \mu_{xx}k_0^2+k_x^2-k^2 & \mu_{xy}k_0^2+k_xk_y & k_xk_z \\ -\mu_{xy}k_0^2+k_xk_y & \mu_{xx}k_0^2+k_y^2-k^2 & k_yk_z \\ k_zk_x & k_zk_y & k_0^2+k_z^2-k^2 \end{vmatrix}=0\ , \tag{7}$$

with

$$k_0^2=\frac{\omega^2}{c^2}\epsilon_{\text{eff}}\ . \tag{7a}$$

Now we discuss two solutions for the two different orientations of the $\mathbf{H}_0$ field [Figs. 1(b) and 1(c)]. In the case where $\mathbf{H}_0$ is parallel to $\hat{\mathbf{n}}$ we obtain from Eq. (7) two modes in which $k_x=k_y=0$ and k_z satisfies the equation $\mu_{xx}k_0^2-k_z^2=\pm i\mu_{xy}k_0^2$. Two roots of these equations are

$$\begin{aligned} k_-^2&=k_0^2(1+4\pi\chi_{\text{res}})\ , \\ k_+^2&=k_0^2(1+4\pi\chi_{\text{nonres}})\ , \end{aligned} \tag{8}$$

where $\chi_{\text{res}}=\chi(\omega-\omega_0)$ and $\chi_{\text{nonres}}=\chi(\omega+\omega_0)$ are the resonance and the nonresonance parts of the susceptibility, respectively. These parts emerge from Eq. (7) if one uses the proper expressions for the components μ_{ik}.[6] In the following we put χ_{nonres} equal to zero. Going back to Eq. (7), we obtain two independent solutions

$$H_\pm=H_x\pm iH_y,\quad E_\pm=\mp\frac{c}{\omega\epsilon_{\text{eff}}}\frac{\partial H_\pm}{\partial z}\ . \tag{9}$$

For a positive g value, the H_- solution represents a field which rotates in the counterclockwise direction and therefore depends upon the resonance part of the magnetization. The other solution does not depend upon the resonance part of the magnetization. In the case of a negative g value H_- and H_+ are interchanged, without an effect on the final results.

In the case where the field $\mathbf{H}_0$ lies in the plane [Fig. 1(c)], we are interested in solutions with $k_x=k_z=0$, $k_y=k\neq 0$. We obtain from Eq. (7) two modes:

$$\begin{aligned} k_a^2&=\frac{\mu_{\text{res}}\mu_{\text{nonres}}}{\mu_{xx}}k_0^2\simeq k_0^2(1+2\pi\chi_{\text{res}})\ , \\ k_b^2&=k_0^2\ . \end{aligned} \tag{10}$$

The approximate expression for k_a^2 in Eq. (10) is obtained if we put[6] $\mu_{\text{nonres}}=1$, $\mu_{xx}\simeq 1+2\pi\chi_{\text{res}}$, and $\mu_{\text{res}}=1+4\pi\chi_{\text{res}}$ and use Eq. (16). For the first mode, Eq. (10), it follows from Eq. (7) that $H_y/H_x=\mu_{xy}/\mu_{xx}$, and this gives, with the help of Eq. (5),

$$B_y=\mu_{yx}H_x+\mu_{yy}H_y=0\ .$$

Therefore the condition $\nabla\cdot\mathbf{B}=0$ and the relevant boundary condition $B_n\,|_{n=0^+}=0$ are automatically fulfilled. Note that a small H_y component which is parallel to the wave vector exists in the medium. The electric field here is transverse and equal to

$$E_z=\frac{c}{\omega\epsilon_{\text{eff}}}k_aH_x\simeq\frac{1}{(\epsilon_{\text{eff}})^{1/2}}(1+2\pi\chi_{\text{res}})^{1/2}H_x\ . \tag{11}$$

The second mode, Eq. (10), does not depend upon the magnetic susceptibility. From Eq. (6) we find that in this mode $\mathbf{H}$ is polarized along the z axis [Fig. 1(c)]. So in the case of the ESR experiment $H_z\,|_{n=0}=0$, and this mode is absent.

Let us compare magnetic losses in both geometries discussed above. The normal component of the Poynting vector, Eq. (2), for the case of Fig. 1(b) may be presented in the form

$$\bar{S}_n=\bar{S}_z=\frac{c}{16\pi}\left[\text{Im}\left[\frac{E_-}{H_-}\right]|H_-|^2-\text{Im}\left[\frac{E_+}{H_+}\right]|H_+|^2\right]\ . \tag{12}$$

According to Eq. (8), only the first term contains the magnetic part of losses. Therefore the relevant impedance here is

$$Z=\frac{c}{16\pi}\text{Im}\left[\frac{E_-}{H_-}\right]\Bigg|_{n=0^+} \tag{13}$$

which is the expression mostly cited and calculated.[3,4] In the case of the in-plane orientation of $\mathbf{H}_0$, we obtain for the magnetic mode ($\mathbf{H}\perp\mathbf{H}_0$)

$$\bar{S}_n=\bar{S}_y=\frac{c}{8\pi}\text{Re}\left[\frac{E_z}{H_x}\right]|H_x|^2\,|_{n=0^+} \tag{14}$$

and

$$Z=\frac{c}{8\pi}\text{Re}\left[\frac{E_z}{H_x}\right]\Bigg|_{n=0^+}\ . \tag{15}$$

To obtain the ESR signal, we need to calculate dZ/dH_0. In the case of small χ_{res} [see Eq. (16)] it is enough to expand Z in terms of χ_{res} and to keep only the linear terms in χ.

Equations (13) and (15) look a bit different, but they lead to the same expression of magnetic losses in our system [Fig. 1(a)] if the condition

$$4\pi|\chi_{\text{res}}|<4\pi\chi_0\frac{H_0}{\Delta H}\ll 1 \tag{16}$$

is fulfilled [here ΔH is the width of the $\chi_{\text{res}}(H_0-H)$ line at half intensity, and χ_0 is the static susceptibility]. Usually Eq. (16) is a good approximation (for 1000 ppm magnetic impurities, with $g=2$, the susceptibility $\chi_0=0.6\times10^{-5}$ for $T=1$ K; $H_0/\Delta H\simeq10^2$–10^3). To point out this similarity we note that (i) the ratios $(E_-/H_-)\,|_{n=0_+}$ and $(E_z/H_x)\,|_{n=0_+}$ are determined by identical conditions of continuity of the in-plane microwave field components (H_- and E_- in the former and E_z and H_x in the latter cases); (ii) the difference with which the magnetic susceptibility χ_{res} influences the wave vector [k_- in the first case, Eq. (8), and k_a in the second, Eq. (10)] is exactly compensated by the factor of 2 in

which Eq. (13) and Eq. (15) are different—note that it is here where we use the condition of Eq. (16):

$$k_- = k_0(1+4\pi\chi_{\rm res})^{1/2} \simeq k_0(1+2\pi\chi_{\rm res})$$

and

$$k_a \simeq k_0 1 + 2\pi\chi_{\rm res} \simeq k_0(1+\pi\chi_{\rm res}) ;$$

(iii) the appearance of Im in Eq. (13) and Re in Eq. (15) is due to the fact that the ratio E_-/H_- has the extra factor of i in comparison with the ratio E_z/H_x [compare Eq. (9) with Eq. (11)]. Also, expressions for the normal component of the Poynting vector, [Eq. (12)] and Eq. (14) give exactly the same result if $4\pi|\chi_{\rm res}| \ll 1$ and the $\mathbf{H}_{\rm real}|_{n=0^-}$ is the same linear polarized field for both cases.

Of course the structure of the fields in our two cases is different. For instance, in the case of the geometry in Fig. 1(c) there is a refraction of the Poynting vector on the upper boundary plane as a result of the presence of the H_y component in the medium. This refraction is a magnetic analogy of the well-known phenomenon of birefringence in optics.

Because we are interested here in the ESR signal only, the geometry of Fig. 1(b) will be used for the derivation of the Z [Eq. (13)]. For simplicity, scalar conductivity (permittivity) is assumed. For some geometries our formulas will be valid also in the case of anisotropic conductivity,[8] for others the anisotropy has to be taken into account from the beginning [Eq. (6)].

B. Specific surface impedance and the line shape of the ESR signal

By using Eqs. (8) and (9) in each of three media of our sandwich [Fig. 1(a)], fields E_- and H_- may be obtained. The impedance Z, Eq. (13), is calculated using the boundary conditions. The procedure is outlined in Appendix A where the following expression is obtained:

$$Z = \frac{c}{16\pi}{\rm Im}\left[\frac{-ick_1}{4\pi\sigma_{1,\rm eff}}\right]\frac{\tan(k_1d_1)+a\tan(k_2d_2)}{1-a\tan(k_1d_1)\tan(k_2d_2)} , \quad (17)$$

where k_i, $i=1,2$ is the wave vector k_- from Eq. (8) for the layer and the substrate, respectively. The metallic-holder conductivity does not appear in Eq. (17) because it is assumed that either $|(\sigma_{2,\rm eff}/\sigma_3)^{1/2}| \ll 1$ in the case of a dielectric substrate or $|k_2d_2| \gg 1$ in the case of a metallic substrate. In the latter case $k_2=(1+i)/\delta_2$, where δ_2 is the skin depth and therefore $\tan(k_2d_2)\simeq i$. In Eq. (17)

$$a = \frac{\sigma_{1,\rm eff}}{\sigma_{2,\rm eff}}\frac{k_2}{k_1}\underset{\chi\to 0}{\longrightarrow}\left[\frac{\sigma_{1,\rm eff}}{\sigma_{2,\rm eff}}\right]^{1/2} \equiv a_0 , \quad (18)$$

where $\sigma_{i,\rm eff}, i=1,2$ is given by Eq. (1) for the layer and the substrate, respectively. From Eq. (8) we obtain

$$k_1 = (k_{01}^2 + 2i\delta_1^{-2})^{1/2} , \quad (19)$$

$$k_2 = (k_{02}^2 + 2i\delta_2^{-2})^{1/2}(1+4\pi\chi_{\rm res})^{1/2} \equiv k_2^0(1+4\pi\chi_{\rm res})^{1/2} , \quad (20)$$

with

$$k_{0i} = \frac{\omega}{c}(\epsilon_i)^{1/2}, \quad \delta_i = c/(2\pi\omega\sigma_i)^{1/2}, \quad i=1,2 . \quad (21)$$

Expanding the surface impedance in $\chi_{\rm res}$ up to linear terms, we obtain from Eq. (17) the magnetic part of the impedance which determines magnetic losses. The ESR line shape will be proportional to the derivative of Z with respect to H_0. If we introduce $Z^{\rm mag} \propto \chi_0$, so that

$$Z = Z(\chi_0=0) + \frac{c}{16\pi}Z^{\rm mag} ,$$

we obtain the following expression:[9]

$$\frac{dZ^{\rm mag}}{dH_0} = {\rm Im}\left[\frac{-ick_2}{4\pi\sigma_{2,\rm eff}}\right][\tan(k_2^0d_2)+k_2^0d_2/\cos^2(k_2^0d_2)]2\pi\phi\frac{d\chi_{\rm res}}{dH_0} , \quad (22)$$

where the function ϕ is equal to

$$\phi = \frac{1}{[\cos(k_1d_1)-a_0\sin(k_1d_1)\tan(k_2^0d_2)]^2} , \quad (23)$$

where a_0 is given by Eq. (18). From Eqs. (22) and (23) it follows that the ESR signal is a mixture of the absorption and of the dispersion parts of the susceptibility $\chi_{\rm res}$. This mixture is determined by the function ϕ which depends upon the ratio of effective conductivities (permittivities) and the ratio d_1/δ_1 of the layer. Such dependence influences the A/B ratio of the ESR signal which may be used for monitoring the layer conductivity and/or the layer thickness. To see how this works it is better to consider the most interesting cases of the metal-metal and semiconductor-insulator systems. The case of a metal-insulator pair is not good for experimental purposes because of the very large differences in the microwave reflectivity of these materials: The parameter a_0 for a metal and a dielectric is equal to $(4\pi\sigma_1/\omega\epsilon)^{1/2}$; for a good metal ($\sigma \sim 3\times 10^{17}$ sec^{-1}) and $\omega = 2\pi\times 10^{10}$ sec, we obtain $a_0 \simeq (4/\sqrt{\epsilon})10^3$, and a crude estimation of Eq. (23) suggests that the metallic layer will diminish the ESR signal from the dielectric by about $|a_0|^2$ ($\sim 10^6$).

C. Metal-metal pair, $|k_2d_2| \gg 1$

In this case $a_0=(\sigma_1/\sigma_2)^{1/2}$, $\tan(k_2^0d_2)\simeq i$, and

$$\phi = \frac{1}{\left[\cos(k_1d_1)-i\left[\frac{\sigma_1}{\sigma_2}\right]^{1/2}\sin(k_1d_1)\right]^2} . \quad (24)$$

From Eq. (22) we obtain

$$\frac{dZ^{\text{mag}}}{dH_0}=\frac{1}{c}\pi\omega\delta_2\left[(\text{Re}\phi+\text{Im}\phi)\frac{d\chi'_{\text{res}}}{dH_0}+(\text{Re}\phi-\text{Im}\phi)\frac{d\chi''_{\text{res}}}{dH_0}\right]. \quad (25)$$

When the layer thickness $d_1\to 0$, $\phi\to 1$ and Eq. (25) gives the usual Dysonian; when $|k_1d_1|\gg 1$, $\phi\simeq 0$ and the signal disappears due to the screening of the substrate by the layer.

The interesting qualitative feature of the line shape, Eq. (25), is the so-called phase reversal of the ESR signal.[2] The normal signal produces the low-field maximum A and the main high-field minimum with its absolute value B [see Fig. 2(a)]. When the mixture coefficient of the absorption part goes through zero [in the case of Eq. (25) it happens when $\text{Re}\phi=\text{Im}\phi$] the signal goes through the symmetrical form (with the maximum A/B ratio) to the phase-reversal form in which the main minimum appears at the low-field side and the maximum A at the high-field side. For $0.2\lesssim\sigma_1/\sigma_2\lesssim 5$ this change of the form occurs at $0.1\lesssim d_1/\delta_2\lesssim 1$. Figure 2 shows the typical signal form, A/B ratio, mixture coefficients from Eq. (25) and intensity parameter $(A+B)(\Delta H)^2$ for the case of a Lorentzian form of $\chi_{\text{res}}(H-H_0)$.

In the case of cylindrical geometry of the cavity, the symmetrical layer-substrate-layer sandwich is the most natural form of the layer-substrate system. If the substrate thickness is larger than the skin depth the line shape of the substrate ESR signal does not differ from the case described above. But in the case where the thickness is of the order of (or less than) the skin depth δ_2, finite thickness of the substrate has to be taken into account. Appendix B deals with the line shape in this case which is relevant to measurements of the diffusion coefficient of the fluorine intercalant in graphite.[8]

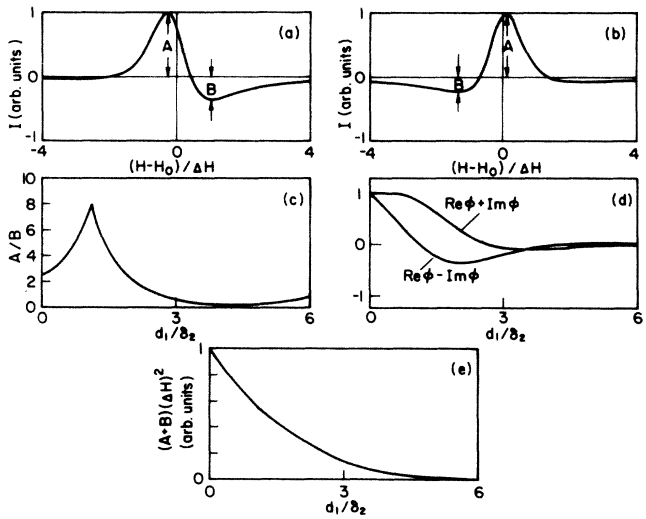

FIG. 2. The theoretical simulation of the ESR of localized spins in the substrate of a metal-metal system. The conductivity ratio $\sigma_1/\sigma_2=0.2$ and the line shape of the $\chi_{\text{res}}(H-H_0)$ function is a Lorentzian. (a) The line shape of the ESR signal for $d_1/\delta_2=0.2$; (b) The line shape with $d_1/\delta_2=1.5$; (c) The A/B ratio as a function of the d_1/δ_2 ratio. The region on the left of the maximum of the curve corresponds to the normal line shape [Fig. 2(a)] and that on its right—to the phase reversal line shape [Fig. 2(b)]. (d) The mixture coefficients from Eq. (25); (e) The intensity parameter $(A+B)(\Delta H)^2$ as a function of d_1/δ_2.

If the layer also contains localized spins which respond to the microwave field, Eqs. (17) and (18) are still valid, but instead of Eq. (19), k_1 now is equal to

$$k_1=(k_1^2+2i\delta_1^{-2})^{1/2}(1+4\pi\chi_{1,\text{res}})^{1/2}. \quad (25a)$$

The ESR signal will now be a superposition of the layer signal and the substrate signal. This is the case reported by Raizman *et al.*,[1] and Appendix C presents the explicit formula for the line shape [Eq. (C1)]. In the case where substrate spins are out of resonance, this formula gives the deformation of the layer signal due to the conductive properties of the substrate.

D. Semiconductor-dielectric pair

This case of the dielectric substrate has an advantage of a simple substrate line shape (absorption only) and the possibility of obtaining very large ESR signals. It is also relatively easy to vary the g factor by choosing appropriate paramagnetic impurities.

To obtain the line shape for the configuration in Fig. 1(a) we substitute $\delta_2^{-1}=0$ in Eq. (20) and preserve the k_{01} in Eq. (19). The k_{01} may be important in semiconductors when $\omega\epsilon_1\simeq\sigma_1$. From Eq. (22) we obtain

$$\frac{dZ^{\text{mag}}}{dH_0}=\frac{2\pi}{(\epsilon_2)^{1/2}}[\tan(k_{02}d_2)+k_{02}d_2/\cos^2(k_{02}d_2)]\times[(\text{Re}\phi)\chi''_{\text{res}}+(\text{Im}\phi)\chi'_{\text{res}}]$$

$$\simeq 8\pi^2\frac{d_2}{\lambda_0}[(\text{Re}\phi)\chi''_{\text{res}}+(\text{Im}\phi)\chi'_{\text{res}}], \quad (26)$$

where the approximate expression in Eq. (26) is for the case $k_{02}d_2\ll 1$, with k_{02} from Eq. (21) (typically $d_2\sim 0.1$ cm, $\lambda_0\sim 1-3$ cm).[9] The function ϕ is now defined by the expression

$$\phi=\frac{1}{[\cos(k_1d_1)-a_0\sin(k_1d_1)\tan(k_{02}d_2)]^2} \quad (27)$$

with a_0 from Eq. (18) and $\sigma_{2,\text{eff}}=-i\omega\epsilon_2/4\pi$. If $d_1\to 0$ the usual ESR absorption signal in a dielectric host is recovered from Eqs. (26) and (27). By introducing $u=(1-v)\cos(k_1d_1)$ and $v=a_0\tan(k_1d_1)\tan(k_2d_2)$, the function ϕ may be written as

$$\phi=[(\text{Re}u)^2-(\text{Im}u)^2-2i\,\text{Re}u\,\text{Im}u]/|\cos(k_1d_1)|^4\times[(1-\text{Re}v)^2+(\text{Im}v)^2]^2. \quad (28)$$

Equation (28) shows that the overall behavior of the ratio A/B in the case of a semiconductor-dielectric pair is analogous to the above-discussed metal-metal case: With an increase of d_1 the ratio starts to rise to a maximum

which occurs when $\mathrm{Im}u = \mathrm{Re}u$ in Eq. (28); after this the phase-reversal form appears and the ratio A/B decreases with further increase of the layer thickness. This behavior is not changed if d_1 is fixed and the conductivity of the layer σ_1 is varied [the A/B ratio depends upon $d_1(\sigma_1)^{1/2}$]. Unlike the metal-metal case, the A/B ratio here is equal to 1 for $d_1(\sigma_1)^{1/2}=0$. Another difference between these two cases may be connected with the function $\chi_{\mathrm{res}}(H_0-H)$. For localized spins in a dielectric, the line shape of the χ_{res} susceptibility is usually not a Lorentzian (see, e.g., our case, Sec. III). Examples of the A/B dependence upon $d_1(\sigma_1)^{1/2}$ are given in the next section in connection with experiments on the Ge-ruby layer-substrate system.

III. EXPERIMENT

A. Selection of materials for the layer-substrate system

The main purpose of this experiment was (i) to demonstrate the possibility of measuring the layer conductivity at microwave frequencies by means of the A/B ratio of the ESR line due to the localized spins in the dielectric substrate and (ii) to develop convenient experimental methods for such measurements.

The dielectric substrate was used because of its simple (a pure absorption form) and high-intensity ESR signal. For the dielectric we chose a ruby crystal (Al_2O_3:Cr^{3+}). The ESR spectrum of Cr^{3+} in this crystal is well known and has been studied extensively in the past.[10] The first derivative of the $\frac{3}{2}\leftrightarrow\frac{1}{2}$ fine-structure transition centered, at approximately 2000 G, is a strong symmetrical line, as shown in Fig. 3. We used this line to monitor the changes in line shape due to a semiconductor layer in a semiconductor-insulator two-layer system.

For the semiconductor layer, n-type Ge (electron concentration of 2.6×10^{14} cm^{-3} at 80 K) was chosen. The Sb doping level in our samples was approximately 10^{14} cm^{-3}. The electrical conductivity of the semiconductor samples was measured using the four-contact method[11] in the temperature range between 290 and 80 K and in magnetic fields relevant to the ESR experiment. The resistivity-temperature relationship at $T>100$ K is characterized by a T^{α} law with α approximately 1.5. This behavior is typical of lattice scattering.[12] Due to the changes in its conductivity with variation of temperature, this semiconductor presents a convenient material in which, by varying the skin depth, one can obtain variations in the line shape (A/B ratio) in the Ge-ruby layer-substrate system. Indeed, the spin depth δ_1 for the relevant angular frequency $\omega\simeq5.73\times10^{10}$ sec^{-1} changes between 540 and 1460 μm in the temperature range 80–290 K. Thus, by varying the temperature, layers of fixed thicknesses up to ~550 μm will cover the most sensitive region of the A/B ratios. The $\frac{3}{2}\leftrightarrow\frac{1}{2}$ ESR transition of Cr^{3+} is not sensitive to the temperature variation within the range mentioned above. So all the temperature-dependent changes of the ESR signal may be ascribed to the Ge conductivity. The Ge permittivity also does not change essentially in this temperature range, but influences k_1 [mostly at room temperature where the ratio $4\pi\sigma_1/\omega\epsilon_1\simeq1.37$ for $\epsilon_1=16$, $\sigma_1=0.127$ $(\Omega\mathrm{cm})^{-1}$, and $\omega=5.73\times10^{10}$ sec^{-1}].

The other advantage of the material used here (n-type Ge) is the small magnetoresistance[13] and the small frequency dependence of the conductivity in the microwave region.[14] After taking into account the small correction of magnetoresistance, a direct comparison between the ac conductivity in the magnetic field of about 2000 G, as obtained from the A/B ratio of the ESR signal, and the dc conductivity measured with the four-contact method is possible. Further we use for permittivities of n-type Ge and ruby the values reported for microwave frequencies $\epsilon_1=16$ (Ref. 15) and $\epsilon_2=10$ (Ref. 16), respectively. Their dispersion in the microwave region may be neglected here.

B. Measurements

Electron-spin resonance measurements were made with a Varian type EC-365 X-band spectrometer, equipped with a Varian E-257 variable-temperature accessory. The temperature was monitored with a copper-Constantan thermocouple connected to a Doric 410A trendicator. A rectangular TE_{012} cavity was used.

A simple sample holder was made from a spectrosil rod, 4 mm in diameter. A flat area was produced at the end of the rod by cutting off part of it with a diamond saw, to accommodate the sample, as shown in Fig. 4. The

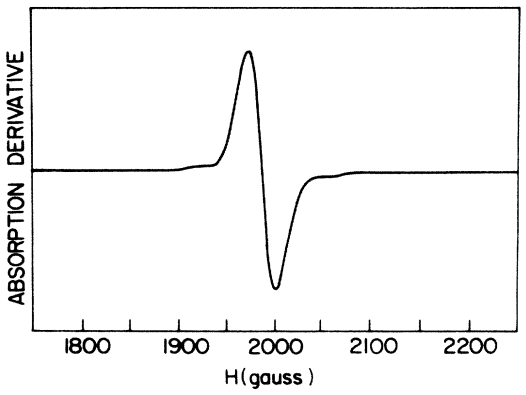

FIG. 3. First derivative of the ESR absorption line of Cr^{3+} in Al_2O_3 ($\frac{3}{2}\leftrightarrow\frac{1}{2}$ fine-structure transition) at room temperature; $f=9.1$ GHz.

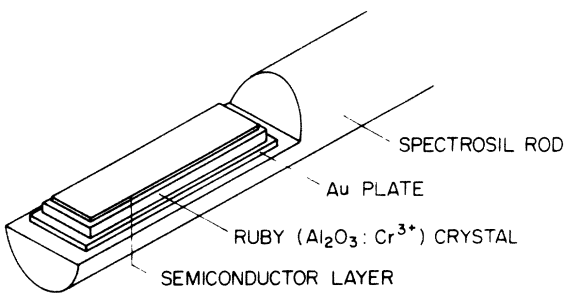

FIG. 4. Spectrosil sample holder with schematic presentation of the mounting of the sample.

ruby crystal was cut to the required size, $\sim 8\times 3.8\times 0.8$ mm^3, with a diamond saw. One flat side of the ruby sample was polished using Diamix diamond polishing compound. The semiconductor crystals were cut to the required size with a wire saw with silicon carbide abrasive; thereafter the samples were polished to the required layer thickness.

The mounting of the sample is shown schematically in Fig. 4. The semiconductor layer was attached to the ruby crystal with wax (LOC-WAX-10). The thickness of the wax layer was between 5 and 25 μm. The ruby was pasted first on a 0.125-mm-thick gold plate which was then pasted on the spectrosil sample holder using Pliobond cement. The gold plate and a cover of silver paint on the exposed edges of the ruby crystal and on the narrow edges of the Ge layer assured that the microwaves would penetrate into the ruby through the semiconductor layer only.

We used n-type Ge layers with $d=250$, 360, and 550 μm. The study of these layers showed the expected overall change in the A/B ratio from values slightly larger than 1 for a thin layer at room temperature (almost insulator type lineshape), through a maximum at some temperature below 100 K (dispersionlike line shape) to a decreasing A/B (reversed-phase line shape; see Secs. II B and II D). An analysis of the ESR line shape of the Cr^{3+} line in ruby showed that it is not a pure Gaussian. To simplify the theoretical calculations we approximated this line shape by a superposition of a Gaussian and Lorentzian, with the same peak-to-peak linewidth of the first derivative of the absorption line. We found that a superposition of 75% Gaussian and 25% Lorentzian gives a good approximation of the experimental lineshape, as shown in Fig. 5. This approximation has to be regarded only as a numerical procedure. (The theoretical line shape should probably be represented by a convolution of a Gaussian and Lorentzian; however, it would have been cumbersome in our case to use this form for numerical calculations.) The maximum A/B ratio is 3.5 for a pure Gaussian and 8 for a pure Lorentzian. For the above superposition we obtained the maximum A/B ratio of approximately 4.5.

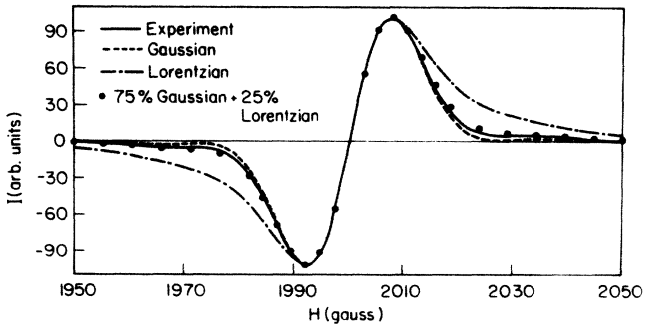

FIG. 5. Approximation of the first derivative of the ESR line of Cr^{3+} in Al_2O_3, by superposition of a Gaussian and Lorentzian. The solid line was plotted from a digitalized form of the experimental trace. The Gaussian, Lorentzian, and their combination, were computed using the same peak-to-peak linewidth as measured in the experiment.

C. Experimental results and layer conductivities

Experimental results were obtained for three n-type Ge layers of various thicknesses. Figures 6(a), 6(b), and 6(c) show the variation of the ESR signal with temperature for the three samples. Clear mixed dispersion-absorption signal line shapes are seen in qualitative agreement with theory.

Figures 7(a), 7(b), and 7(c) give a comparison of the experimental A/B ratios, as a function of d_1/δ_1, with the theoretical curve for the appropriate layer thickness. The theoretical curves of the A/B ratios were computed using Eqs. (26), (18)—(21), and (27) with the parameters pointed out in the figures. The theoretical ϕ curve of Eq. (27) is presented in Fig. 8. For each point d_1/δ_1, the conductivity σ_1 was calculated and substituted into Eqs. (18)—(21). The $\chi_{\rm res}(H-H_0)$ is approximated by a superposition of a Gaussian and Lorentzian (see Fig. 5):

$$\chi_{\rm res}=C[0.75\chi_{\rm Gauss}(x)+0.25\chi_{\rm Lorentz}(x)] ,$$

where C is a constant proportional to the static susceptibility of the localized spins χ_0 and $\chi_{\rm Gauss}(x)$ (Ref. 17), and $\chi_{\rm Lorentz}(x)$ are

$$\chi''_{\rm Gauss}(x)=e^{1/2}e^{-x^2/2} ,$$
$$\chi'_{\rm Gauss}(x)=e^{1/2}\frac{2}{\sqrt{\pi}}e^{-x^2/2}\int_0^{x/\sqrt{2}}e^{u^2}du , \tag{29}$$
$$\chi''_{\rm Lorentz}(x)=\frac{8}{3+x^2},\quad \chi'_{\rm Lorentz}(x)=\frac{8}{\sqrt{3}}\frac{x}{3+x^2} ,$$

$x=(H-H_0)/\frac{1}{2}\Delta H_{\rm p.p.}$. $\Delta H_{\rm p.p.}$ is the peak-to-peak linewidth of the first derivative of the absorption line taken to be the same for the Gaussian and the Lorentzian. The expression for $\chi'_{\rm Gauss}(x)$ is valid for $\Delta H_{\rm p.p.}/H_0 \ll 1$.[17] This condition holds in our case; see Fig. 3.

The experimental values of A/B were extracted from ESR traces and the corresponding d_1/δ_1 values were calculated using the resistivity ρ measured by the four-contact method, also taking into account the small magnetoresistance.[13] The errors in the measurements of the A/B ratios are larger in the vicinity of the peak of the A/B versus d_1/δ_1 curve and beyond it, in the region characterized by phase-reversed line shape. The maximum error detected for A/B in our experiments was $\sim 15\%$. The resistivity measurements exhibited a spread of ρ values between its minimum and maximum of approximately $\pm 18\%$.

It can be seen in Figs. 7(a), 7(b), and 7(c) that a good fit was obtained between the experimental A/B values versus $d_1/\delta_1\{=\text{const}[d_1(\sigma_1)^{1/2}]\}$ and the theoretically calculated ones. In view of the idealized geometry used for the theoretical calculations and the spread of the experimental points, one can consider the agreement very good.

IV. DISCUSSION AND CONCLUSION

The method suggested here may have various possible applications.

(i) A layer-substrate system may occur naturally either as a result of some treatment of samples[1,2] or because of the slow diffusion of some atoms in a substrate[8] or be

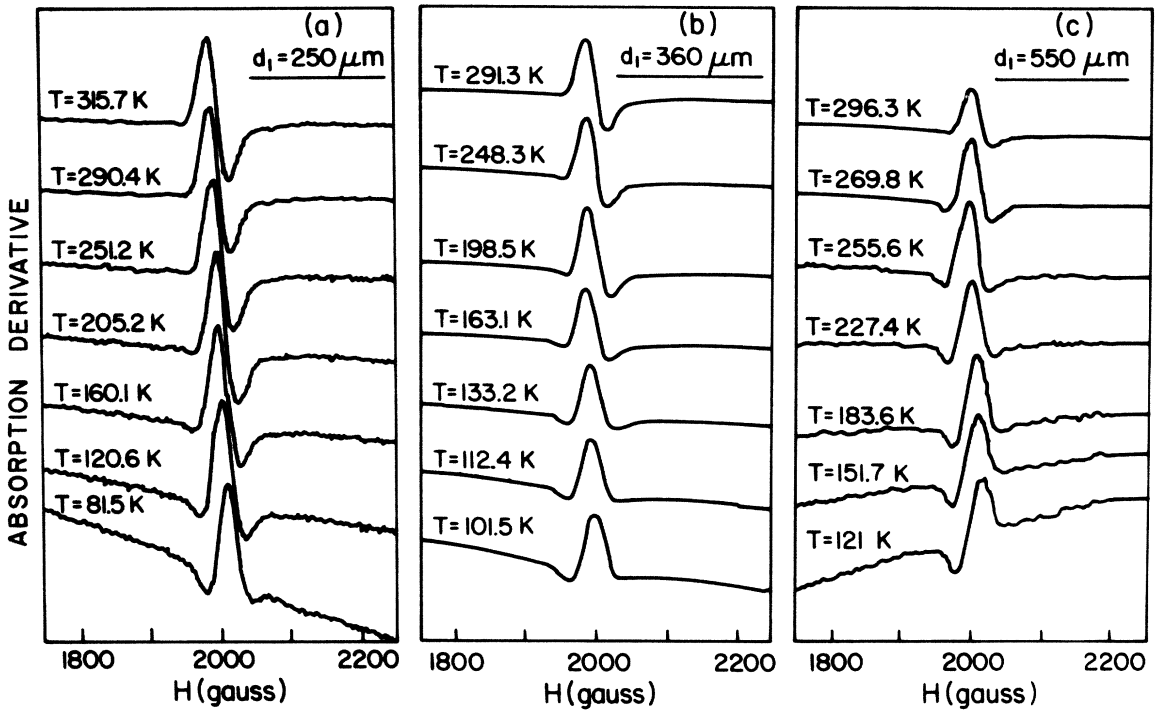

FIG. 6. Variation of the ESR line shape (A/B ratio) of Cr^{3+} in Al_2O_3 with temperature, in a two-layer Ge-ruby structure, for various thicknesses d_1 of the Ge layer. The thickness of the ruby substrate was $d_2 = 690\ \mu m$ in the case (b) and 675 μm in the two other cases (a) and (c). (a) $d_1 = 250\ \mu m$, $f = 9.11$ GHz, (b) $d_1 = 360\ \mu m$, $f = 9.12$ GHz, (c) $d_1 = 550\ \mu m$, $f = 9.12$ GHz.

prepared artificially in the course of building an electronic device. In these cases ESR of localized spins of the substrate and/or the layer may be used to study the process of the layer formation and its conductivity properties. In particular, the diffusion coefficient may be measured by means of the A/B ratio of the ESR signal because the thickness of the layer in the diffusion process will change with time, resulting in a corresponding time dependence of the ESR line shape.[8] If the ESR signal is due to substrate spins only, formulas of Sec. II or Appendix B are valid.[8] If the ESR is due to layer spins or both layer and substrate spins, formulas of Appendix C could be used. Of course, the latter treatment is much more cumbersome.

(ii) The main aim of this study was to develop a new way of measuring the ac conductivity and/or the thickness of conductivity layers by means of the deformation of the substrate ESR signal. At first sight it is very indirect and roundabout way to measure conductivity. This is true when the usual electrical (contact) method is available. However, there are cases when measurement of elec-

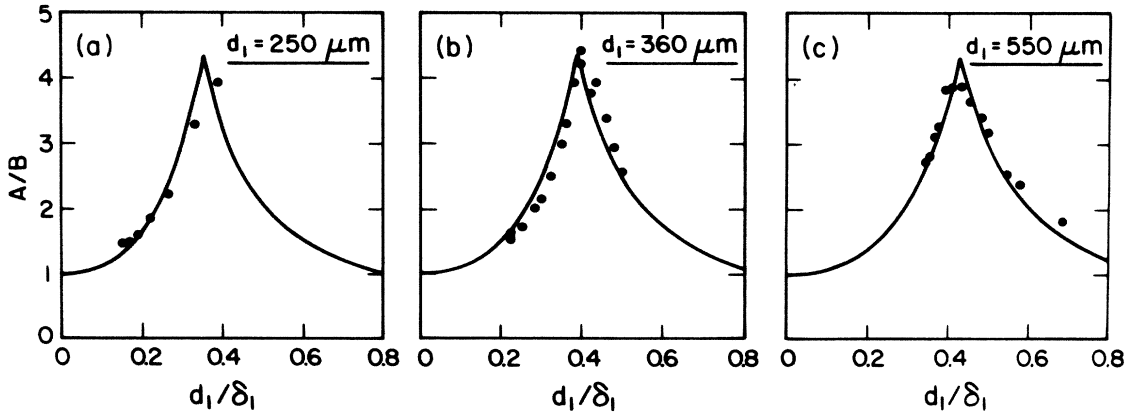

FIG. 7. The A/B ratio vs d_1/δ_1. The solid lines were theoretically calculated. The experimental points, represented by circles, were extracted from the traces shown in Fig. 6, as well as from other traces (not shown) obtained from these two-layer structures. (a) $d_1 = 250\ \mu m$, (b) $d_1 = 360\ \mu m$, (c) $d_1 = 550\ \mu m$.

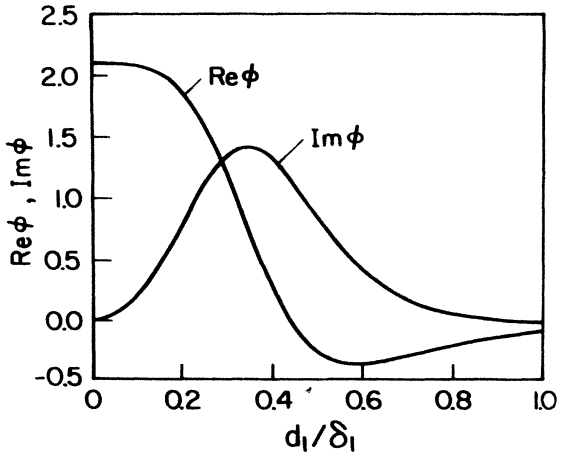

FIG. 8. Reϕ and Imϕ vs d_1/δ_1 [Eq. (27)] for the Ge-ruby system. $\epsilon_1=16$, $\epsilon_2=10$, $\omega=0.573\times10^{11}$ sec^{-1}, $d_1=0.036$ cm, $d_2=0.069$ cm.

trical conductivity poses a severe experimental problem. In these cases the method suggested here may be very useful.

Nowadays studies of the metal-insulator transitions and the conductivity percolation are very timely. The measuring of the ac conductivity in these layer systems provide a convenient supporting study of phase transitions.

The method has its limitations. The most important of them are (i) low sensitivity for layer thicknesses which are either larger or much less than the skin depth and (ii) the necessity of the presence of the constant magnetic field. The second one may sometimes not be essential—as in the case of the Ge layer reported here. There are many materials with a small magnetoresistance effect. In principle, the influence of the magnetic field on the conductivity in this method may be eliminated by using the zero-field ESR.[18] In the zero-field ESR appropriate crystal-field levels of paramagnetic ions are used for ESR transitions in the microwave region. Another expansion of this method may be considered in the direction of much small frequencies.

In this work the conductivity of the Ge semiconductor layer was changed by varying the temperature. The method may be very useful when the conductivity is changed by irradiation with light. Thus, the ESR of the dielectric substrate may be used for monitoring the photoeffect in semiconducting layers. Another challenging application of this method may be a study of properties of superconducting films, such as penetration depth.

The CESR of the metal substrate may be also used for the monitoring of the conductivity of the layer. However, the theoretical formulas are much more cumbersome because of the presence of the magnetization diffusion and sometimes also the anomalous skin effect. In the case of local spins the initial line shape of the substrate ESR signal is much simpler than in the CESR, and the intensity of the signal is greater, especially for an insulator substrate. Besides, the overlap between the CESR of the layer and the CESR of the metallic substrate is sometimes difficult to avoid because of the closeness of conduction electron g factors in different metals.[19] On the other hand, the transition mode of the CESR is a very useful tool for the study of other aspects of two-layer systems.[20,21]

In summary, in this paper we suggest a new method monitoring the conductivity and/or the thickness of a semiconducting or conducting layer by means of ESR of local spins of the substrate; in particular, the semiconducting layer on the dielectric substrate system was studied theoretically and experimentally. The experiments on the Ge-ruby system are described here, and the validity of the method is shown. Another example of the usefulness of the method is demonstrated in Ref. 8. The possible applications of the method are discussed.

ACKNOWLEDGMENTS

We are indebted to Professor D. Shaltiel for many discussions, especially in the first stages of the work. We thank Dr. A. Zemel for many discussions and for the four-contact measurements and Dr. S. Rotter for assistance in the treatment of materials used here. We thank Ms. D. Goldwirt and Mr. G. Polatsek for programming of the computational part of this work and Dr. F. Mustachi and Mr. M. Azoulay for the ruby and Ge crystals, respectively. This work was supported by the Basic Research Foundation administered by the Israel Academy of Sciences and Humanities.

APPENDIX A: CALCULATION OF SURFACE IMPEDANCE

Here we present details of the calculations of the surface impedance, Eq. (17). The geometry of Fig. 1(b) is assumed. All general formulas and definitions are in Sec. II.

For the layer (metal, semiconductor),

$$H_-=(h_1e^{ik_1z}+h_2e^{-ik_1z})e^{-i\omega t},$$
$$E_-=\frac{ck_1}{4\pi\sigma_{1,\text{eff}}}(h_1e^{ik_1z}-h_2e^{-ik_1z})e^{-i\omega t}, \tag{A1}$$

where $k_1\equiv k_{-1}$ from Eq. (8). In the case where the resonance magnetization of the layer is absent

$$k_1=\frac{\omega}{c}(\epsilon_{1,\text{eff}})^{1/2}, \tag{A2}$$

where ϵ_{eff} and σ_{eff} are defined in Eq. (3) and Eq. (1), respectively.

For the substrate (metal, semiconductor, dielectric),

$$H_-=(h_3e^{ik_2(z-d_1)}+h_4e^{-ik_2(z-d_1)})e^{-i\omega t},$$
$$E_-=\frac{ck_2}{4\pi\sigma_{2,\text{eff}}}(h_3e^{ik_2(z-d_1)}-h_4e^{-ik_2(z-d_1)})e^{-i\omega t}, \tag{A3}$$

where $k_2\equiv k_{-2}$ from Eq. (8).

For the thick metal,

$$H_-=h_5e^{ik_3(z-d_2)}e^{-i\omega t},$$
$$E_-=\frac{ck_3}{4\pi\sigma_3}e^{ik_3(z-d_2)}e^{-i\omega t}, \tag{A4}$$

$$k_3=\frac{1+i}{\delta_3}\ ,$$

where δ_3 is the skin depth of the thick metal.

For the boundary conditions [Fig. 1(a)], the upper boundary plane is

$$h_1+h_2=H_-\,|_{n=0^-}=H_x^0\ ,$$

$$\frac{ck_1}{4\pi\sigma_{1,\mathrm{eff}}}(h_1-h_2)=E_-\,|_{n=0^-}\ ,$$

the middle boundary plane is

$$h_1e^{ik_1d_1}+h_2e^{-ik_2d_2}=h_3+h_4\ ,$$

$$\frac{k_1}{\sigma_{1,\mathrm{eff}}}(h_1e^{ik_1d_1}-h_2e^{-ik_2d_2})=\frac{k_2}{\sigma_{2,\mathrm{eff}}}(h_3-h_4)\ ,$$

and the lower boundary plane is

$$h_3e^{ik_2d_2}+h_4e^{-ik_2d_2}=h_5\ ,$$

$$h_3e^{ik_2d_2}-h_4e^{-ik_2d_2}=\alpha_{23}h_5\ ,$$

$$a_{23}=\left[\frac{\sigma_{2,\mathrm{eff}}}{\sigma_3}\right]^{1/2}\ .$$

We find

$$\begin{aligned}h_1&=\tfrac{1}{4}[(1+a)(1+a_{23})e^{-ik_2d_2}\\&\quad+(1-a)(1-a_{23})e^{ik_2d_2}]e^{-ik_1d_1}h_5\ ,\\h_2&=\tfrac{1}{4}[(1-a)(1+a_{23})e^{-ik_2d_2}\\&\quad+(1+a)(1-a_{23})e^{ik_2d_2}]e^{ik_1d_1}h_5\ ,\\a&=\frac{\sigma_{1,\mathrm{eff}}}{\sigma_{2,\mathrm{eff}}}\frac{k_2}{k_1}\ ,\end{aligned}\tag{A5}$$

usually either $|a_{23}|\ll 1$ (metal-dielectric boundary) or $d_2\gg\delta_2$. For both cases we obtain from Eq. (A5), neglecting a_{23}, the surface impedance for our mode:

$$\begin{aligned}Z&=\frac{c}{16\pi}\mathrm{Im}\left[\frac{E_-}{H_-}\right]\Bigg|_{n=0^+}\\&=\frac{c}{16\pi}\mathrm{Im}\frac{(-i)ck_1}{4\pi\sigma_{1,\mathrm{eff}}}\frac{\tan(k_1d_1)+a\tan(k_2d_2)}{1-a\tan(k_1d_1)\tan(k_2d_2)}\ ,\end{aligned}$$

which we use in Sec. II [Eq. (17)].

The magnetic losses which are proportional to the susceptibility may also be calculated directly from the expression[6]

$$Q=\frac{1}{4\pi}\int dV\,\overline{\mathbf{H}_{\mathrm{real}}\cdot\mathbf{B}_{\mathrm{real}}}+\frac{1}{4\pi}\overline{\int dV\,\mathbf{E}_{\mathrm{real}}\cdot\mathbf{D}_{\mathrm{real}}}\tag{A6}$$

after expending Q from Eq. (A6) in χ. This way of calculating is much more laborious than surface impedance calculations, however it gives an interesting energetical insight into the ESR line shape. We will demonstrate this point for the case of the thick metal only (localized spins ESR in metals). It is easy to see that

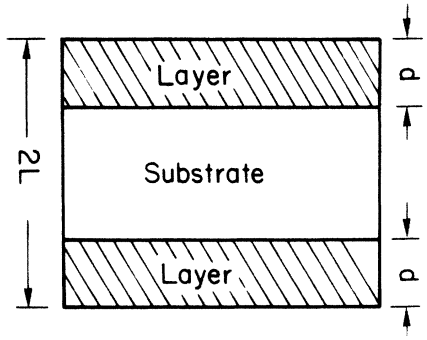

FIG. 9. The layer-substrate-layer geometry.

$$\overline{\mathbf{H}_{\mathrm{real}}\cdot\mathbf{B}_{\mathrm{real}}}=\frac{\omega}{2}\mathrm{Im}(\mathbf{H}\cdot\mathbf{B})$$

and analogically for the electrical component. Using $B_-=\mu_{\mathrm{res}}H_-$, $B_+=\mu_{\mathrm{nonres}}H_+$, $D_\pm=\epsilon_{\mathrm{eff}}E_\pm$, and Eq. (A1), one finds

$$\begin{aligned}Q&=Q_1+Q_2\ ,\\Q_1&=\frac{\omega\delta}{8}\chi''_{\mathrm{res}}H_x^{02}\ ,\end{aligned}\tag{A7}$$

$$Q_2=\left[\frac{\omega\delta}{16\pi}+\frac{\omega\delta}{16}(\chi'_{\mathrm{res}}-\chi''_{\mathrm{res}})\right]H_x^{02}\ ,\tag{A8}$$

where Q_1 and Q_2 are the first and second terms in Eq. (A6), respectively.

Magnetic losses are equal to

$$\frac{\omega\delta}{16}(\chi'_{\mathrm{res}}+\chi''_{\mathrm{res}})H_x^{02}$$

and give rise to the Dysonian line shape. However, these magnetic losses are composed of the direct magnetic losses $\sim\chi''_{\mathrm{res}}$, Eq. (A7), and the electrical losses $\propto\frac{1}{2}(\chi'_{\mathrm{res}}-\chi''_{\mathrm{res}})$, Eq. (A8). The last is obvious because the skin depth depends upon the magnetic permeability.

APPENDIX B: THE CASE OF THE LAYER-SUBSTRATE-LAYER SANDWICH

In the case of the cylindrical cavity a sample with a symmetrical plane geometry is more suitable. For this case we consider a layer-substrate system, as shown in Fig. 9, with symmetrical upper and lower boundaries. The microwave magnetic field in the sample now is symmetric and the electric field is antisymmetric relative to the middle plane. By means of boundary conditions outlined in Appendix A, we obtain instead of Eq. (17) the following expression:

$$Z=\frac{c}{16\pi}\mathrm{Im}\left[\frac{-ck_1}{4\pi\sigma_{1,\mathrm{eff}}}\right]\frac{\tan(k_1d_1)+a\tan[k_2(L-d_1)]}{1-a\tan(k_1d_1)\tan[k_2(L-d_1)]}\ ,\tag{B1}$$

with the same meaning of parameters. For the meaning of L, see Fig. 9. Also Eq. (25) for a metal-metal case preserves its form, but instead of the function ϕ in Eq. (24), we obtain a new function

$$\tilde{\phi}=\frac{-i\left[\frac{\sigma_2}{\sigma_1}\right]^{1/2}X(L,d_1)\{1+2k_2^0(L-d_2)/\sin[2k_2^0(L-d_1)]\}}{[\cos(k_1d_1)-X(L,d_1)\sin(k_1d_1)]^2}, \tag{B2}$$

with

$$X(L,d_1)=\left[\frac{\sigma_1}{\sigma_2}\right]^{1/2}\tan[k_2^0(L-d_1)]\underset{L\to\infty}{\to} i\left[\frac{\sigma_1}{\sigma_2}\right]^{1/2}. \tag{B3}$$

From Eqs. (B2) and (B3), the function $\tilde{\phi}$ in the limit $L\to\infty$ becomes the function ϕ from Eq. (24). The ESR line shape of this geometry will not be quantitatively different from the line shape discussed in Sec. II C if $(L-d_1)$ will be of the order of the skin depth δ_2. Qualitatively the A/B ratio as a function of d_1/δ_2 behaves the same as discussed in Sec. II C.

APPENDIX C: THE CASE WHERE BOTH THE LAYER AND SUBSTRATE CONTAIN LOCALIZED SPINS

In Ref. 1 we discussed the line shape of the ESR signal in the case where both the metallic layer and the metallic substrate possess localized spins. The geometry of Fig. 1(a) is assumed. In this case Eq. (17) is still valid (with $\tan(k_2d_2)\simeq i$) but k_1 is given now by Eq. (25a). Expanding both k_2 and k_1 up to linear terms in their susceptibilities, we obtain that the ESR signal is a superposition of the layer and substrate signals:[1]

$$\frac{dZ}{dH_0}\propto\delta_1\left[C_1\frac{d\chi_1''(H_0)}{dH_0}+C_2\frac{d\chi_1'(H_0)}{dH_0}\right]+\delta_2\left[C_3\frac{d\chi_2''(H_0)}{dH_0}+C_4\frac{d\chi_2'(H_0)}{dH_0}\right], \tag{C1}$$

where indices 1 and 2 are for the layer and the substrate, respectively. The substrate signal is defined by Eq. (25), e.g., $C_3=\mathrm{Re}\phi-\mathrm{Im}\phi$, $C_4=\mathrm{Re}\phi+\mathrm{Im}\phi$, with ϕ from Eq. (24). The explicit form of the layer signal is

$$C_1=\mathrm{Re}f_1,\quad C_2=\mathrm{Im}f_1, \tag{C2}$$

where

$$f_1=2x[(\cosh^{-2}x'+\tanh x'/x')]\Big/\left[\left[\frac{\sigma_1}{\sigma_2}\right]^{1/2}\tanh x'+1\right]-\frac{\sigma_1}{\sigma_2}\left\{\left[\left[\frac{\sigma_2}{\sigma_1}\right]^{1/2}\tanh x'+1\right](\cosh^{-2}x'-\tanh x'/x')\Big/\left[\left[\frac{\sigma_1}{\sigma_2}\right]^{1/2}\tanh x'+1\right]^2\right\}, \tag{C3}$$

where $x'=(1+i)x$, $x=d_1/\delta_2$. These results were used in Refs. 1 and 2.

[1] A. Raizman, J. T. Suss, D. N. Seidman, D. Shaltiel, and V. Zevin, Phys. Rev. Lett. **46**, 141 (1981).

[2] A. Raizman, J. T. Suss, D. N. Seidman, D. Shaltiel, and V. Zevin, Physica **107B**, 357 (1981).

[3] J. Winter, *Magnetic Resonance in Metals* (Clarendon, Oxford, 1971), Chap. 10.

[4] J. M. Pifer and R. Magno, Phys. Rev. B **3**, 663 (1971); I. Zamaleev, A. Kessel, G. Teitelbaum, and E. Kharakhashian, Fiz. Met. Metalloved. **34**, 16 (1972).

[5] M. Lampe and P. M. Platzman, Phys. Rev. **150**, 350 (1966).

[6] R. White, *The Quantum Theory of Magnetism* (Springer, Berlin, 1983), Chap. 5.

[7] L. Landau, E. Lifshitz, and L. Piteevskii, *Electrodynamics of Continuous Media* (Pergamon, New York, 1983).

[8] I. Palachan, D. Davidov, V. Zevin, G. Polatsek, and H. Selig, Phys. Rev. B **32**, 5554 (1985).

[9] If $k_{02}d_2\sim\pi/2$ the expansion, Eq. (22), is not valid. Here we are interested only in cases for which $k_{02}d_2<1$.

[10] A. Manenkov and A. Prokhorov, Zh. Eksp. Teor. Fiz. **28**, 764 (1955) [Sov. Phys.—JETP **1**, 611 (1955)]; J. E. Geusik, Phys. Rev. **102**, 1252 (1956); M. M. Zaripov and Iu. Ia. Shamonin, Zh. Eksp. Teor. Fiz. **30**, 291 (1956) [Sov. Phys.—JETP **3**, 171 (1956)].

[11] L. J. van der Pauw, Philips Res. Rep. **13**, 1 (1958).

[12] R. A. Smith, *Semiconductors* (Cambridge University Press, Cambridge, England, 1961).

[13] The magnetoresistance $\Delta\rho/\rho$ of a typical Ge sample at 2000 G increased from 0.4% at room temperature to 6.8% at 95 K.

[14] The effective (average) mass of the conduction electron is $0.22m_0$ (see Ref. 12, p. 347). For $T=80$ K we obtain ($\sigma=0.68\ \Omega^{-1}\mathrm{cm}^{-1}$, $n=2.6\times10^{14}\ \mathrm{cm}^{-3}$) $\omega\tau\simeq0.13$ for $\omega=0.57\times10^{12}\ \mathrm{sec}^{-1}$.

[15] *Physics of II-IV and I-VII Compounds, Semimagnetic Semiconductors*, Vol. 17, Teil b of *Landolt-Börnstein*, edited by O. Madelung, M. Schultz, and M. Weiss (Springer, Berlin, 1982), p. 114.

[16] *American Institute of Physics Handbook*, edited by D. E. Gray, (McGraw-Hill, New York, 1962), pp. 9–109.

[17] G. E. Pake and N. Purcell, Phys. Rev. **74**, 1184 (1948); **75**, 534 (1949).

[18] G. S. Bogle and M. F. Symmons, Proc. R. Soc. London **79**, 775 (1963); M. M. L. Pryce and K. W. H. Stevens, Proc. Phys. Soc. London, Sect. A **63**, 36 (1951).

[19] When the CESR of the layer is not interfering with the substrate CESR [see for instance, I. Palchan, F. Mustachi, D. Davidov, and M. Selig, Synth. Met. **10**, 101 (1984)] the substrate still influences—if $d_1\lesssim\delta_1$—the layer CESR by its conductivity. Therefore the CESR of the layer on the conducting substrate will be different from the thin film case in Ref. 4.

[20] D. C. Vier, D. W. Tolleth, and S. Schultz, Phys. Rev. B **29**, 88 (1984).

[21] The line shape of the CESR in inhomogeneous medium was theoretically considered by H. H. Hurdequint, thesis, Universite de Paris-Sud, Orsay, 1981.